

NAVAL POSTGRADUATE SCHOOL MONTEREY CALIF F/G 4/2  
OBSERVATIONS OF THE TEMPERATURE STRUCTURE FUNCTION PARAMETER, C--ETC(U)  
SEP 78 K L DAVIDSON, T M HOULIHAN  
NPS-63DS78005 NL

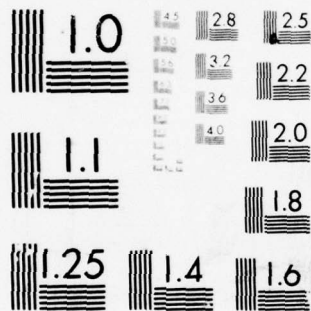
F/G 4/2

NL

1 OF 1  
AD  
A061283

END  
DATE  
FILMED  
2 - 79  
DDC

2 - 79



MICROCOPY RESOLUTION TEST CHART  
NATIONAL BUREAU OF STANDARDS-1963-A

LEVEL II

*P*  
NW

NPS63-78-005

NAVAL POSTGRADUATE SCHOOL  
Monterey, California

AD A061283

DDC FILE COPY



DDC  
RECEIVED  
NOV 17 1978  
D

OBSERVATIONS OF THE TEMPERATURE STRUCTURE  
FUNCTION PARAMETER,  $C_T^2$ , OVER THE OCEAN

K. L. Davidson, T. M. Houlihan,  
C. W. Fairall, and G. E. Schacher

September 1978

Approved for public release; distribution  
unlimited. Reproduction in whole or in part  
is permitted for any purpose of the United  
States Government.

78 11 13 082

NAVAL POSTGRADUATE SCHOOL  
Monterey, California

Rear Admiral T.W. Dedman  
Superintendent

J.R. Borsting  
Provost

The work reported herein was supported in part by the  
Naval Ocean Systems Center (EOMET).

Reproduction of all or part of this report is authorized.

This report was prepared by:

K.L. Davidson  
K.L. Davidson  
Associate Professor of  
Meteorology

G.E. Schacher  
G.E. Schacher  
Associate Professor of Physics

C.W. Fairall  
C.W. Fairall  
Assistant Professor of  
Physics

T.M. Houlihan  
T.M. Houlihan  
Associate Professor of  
Mechanical Engineering

Approved by:

G. J. Haltiner  
G. Haltiner, Chairman  
Department of Meteorology

William M. Tolles  
William M. Tolles  
Dean of Research



UNCLASSIFIED

SECURITY CLASSIFICATION OF THIS PAGE (When Data Entered)

REPORT DOCUMENTATION PAGE		READ INSTRUCTIONS BEFORE COMPLETING FORM
1. REPORT NUMBER 14 NPS-63Ds78005	2. GOVT ACCESSION NO.	3. RECIPIENT'S CATALOG NUMBER (9)
4. TITLE (and Subtitle) OBSERVATIONS OF THE TEMPERATURE STRUCTURE FUNCTION PARAMETER, $C_T^2$ , OVER THE OCEAN		5. TYPE OF REPORT & PERIOD COVERED Oct 1977 - Oct 1978
7. AUTHOR(s) 10 K. L. Davidson, T. M. Houlihan, C. W. Fairall, and G. E. Schacher		6. PERFORMING ORG. REPORT NUMBER
9. PERFORMING ORGANIZATION NAME AND ADDRESS Naval Postgraduate School Monterey, CA 93940		8. CONTRACT OR GRANT NUMBER(s) N00019-78-WR-81002 N66001-78-WR-00156
11. CONTROLLING OFFICE NAME AND ADDRESS Naval Oceans Systems Center San Diego, CA 92152		10. PROGRAM ELEMENT, PROJECT, TASK AREA & WORK UNIT NUMBERS (12) 45p
14. MONITORING AGENCY NAME & ADDRESS (if different from Controlling Office)		12. REPORT DATE (11) September 1978
		13. NUMBER OF PAGES 45
		15. SECURITY CLASS. (of this report) UNCLASSIFIED
		15a. DECLASSIFICATION/DOWNGRADING SCHEDULE
16. DISTRIBUTION STATEMENT (of this Report) Approved for public release; distribution unlimited. Reproduction in whole or in part is permitted for any purpose of the United States Government.		
17. DISTRIBUTION STATEMENT (of the abstract entered in Block 20, if different from Report)		
18. SUPPLEMENTARY NOTES		
19. KEY WORDS (Continue on reverse side if necessary and identify by block number) Temperature structure, Boundary layer, Turbulence  (C sub T) squared		
20. ABSTRACT (Continue on reverse side if necessary and identify by block number) Observational results from shipboard measurements of temperature fluctuations, and mean wind, temperature, and humidity, are com- pared with existing expressions for the surface flux and height dependence of $C_T^2$ . Surface flux estimates are obtained from bulk aerodynamic formulae. Temperature fluctuation data are selected to minimize a salt-contamination effect which causes increases in temperature variance. Predictions for $C_T^2$ based on surface flux scaling agree within 20%, except for near neutral and large		

DD FORM 1 JAN 73 1473

EDITION OF 1 NOV 68 IS OBSOLETE  
S/N 0102-014-6601

UNCLASSIFIED

SECURITY CLASSIFICATION OF THIS PAGE (When Data Entered)

251 450 78 11 13 082

UNCLASSIFIED

SECURITY CLASSIFICATION OF THIS PAGE(When Data Entered)

unstable conditions where the disagreement can be attributed to measurement problems.

ACCESSION NO.	
NTIS	Write Section <input checked="" type="checkbox"/>
DDO	Self Section <input type="checkbox"/>
UNANNOUNCED	<input type="checkbox"/>
JUSTIFICATION.....	
BY.....	
DISTRIBUTION/AVAILABILITY CODES	
Dist. AVAIL. and/or SPECIAL	
A	

UNCLASSIFIED

SECURITY CLASSIFICATION OF THIS PAGE(When Data Entered)

## Table of Contents

INTRODUCTION .....	1
SURFACE LAYER BULK AERODYNAMIC RELATIONS FOR $C_T^2$ .....	3
EXPERIMENTAL ARRANGEMENTS .....	7
DATA EVALUATION AND ERROR ANALYSIS .....	9
RESULTS .....	13
CONCLUSIONS .....	17
ACKNOWLEDGEMENTS .....	18
REFERENCES .....	19
LIST OF TABLES .....	21
LIST OF FIGURES .....	26

Observations of the temperature structure function  
parameter,  $C_T^2$ , over the ocean

K. L. Davidson, T. M. Houlihan, C. W. Fairall and  
G. E. Schacher

Environmental Physics Group  
Naval Postgraduate School  
Monterey, CA 93940

Abstract

Observational results from shipboard measurements of temperature fluctuations, and mean wind, temperature, and humidity, are compared with existing expression for the surface flux and height dependence of  $C_T^2$ . Surface flux estimates are obtained from bulk aerodynamic formula. Temperature fluctuation data are selected to minimize a salt-contamination effect which causes increases in temperature variance. Predictions for  $C_T^2$  based on surface flux scaling agree within 20%, except for near neutral and large unstable conditions where the disagreement can be attributed to measurement problems.



## 1. Introduction

The atmospheric marine surface layer is that region in the first 50 meters or so over the sea which is characterized by large turbulent vertical transfer of momentum, heat, and moisture. Progress has been made in specifications of surface wind fields and hydrostatic stability for this region since these are parameters used in estimating boundary fluxes in numerical atmospheric prediction and for predicting changes in the upper part of the ocean. Another interest in this region is the quantification of turbulent effects on optical wave propagation. The optical effects occur at scales which are smaller than those associated with boundary fluxes. This involves specifications of fluctuations in velocity, temperature, and humidity for scales approaching those responsible for viscous dissipation of turbulent kinetic energy and molecular diffusion of scalar (temperature and humidity) quantities.

Existing measurement capabilities and turbulence theory enable observations of the small scale properties of interest, but the complexities and cost of such direct observations inhibit them on routine bases. Therefore, there is a need to examine relationships between the small scale properties and the more feasibly measured parameters: the mean winds, temperature, and humidity.

Descriptions of the small scale turbulent properties have not been as complete nor in the quantity for the overwater regime as for the overland regime (described by Champagne, et al., 1977). The overwater regime requires separate considera-

tion because of evidence of influence on the airflow by the surface waves (Davidson, 1974) and the importance of the water vapor content of the air. The water vapor effects are manifested both in atmospheric stability and in optical propagation.

For optical waves, the largest contributors to the refractive-index fluctuations are temperature fluctuations ( $T'$ ). Friehe, et al. (1975) have shown that another significant contributor may be the temperature-humidity fluctuation covariance. They observed a contribution of 24% to the refractive index structure function parameter,  $C_n^2$ , from humidity effects during a time when the temperature-humidity covariance was positive.

The intensity of temperature fluctuations for scales from a few millimeters to several meters can be characterized by the temperature structure function parameter,  $C_T^2$ , defined as

$$C_T^2 = \frac{D_T(r)}{r^{2/3}} \quad (1)$$

$D_T(r)$  is defined as  $D_T(r) = \overline{[T(x) - T(x+r)]^2}$  where  $T(x)$  and  $T(x+r)$  are temperature at two points on a line oriented normal to the mean wind direction separated by the distance  $r$ .

The temperature structure function parameter can also be related to small scale processes of turbulent kinetic energy dissipation and heat diffusion by the following expression

$$C_T^2 = \eta \epsilon^{-1/3} \chi \quad (2)$$

where  $\eta$  is a constant equal to 3.2,  $\epsilon$  is the dissipation rate of turbulent kinetic energy and  $\chi$  is the rate at which the temperature inhomogeneities are diffused or "smeared" out. Equation 2 arises from two parallel expressions for the one-dimensional variance spectrum for temperature fluctuations in the inertial subrange.

$$S_T(k) = \alpha C_T^2 k^{-5/3} \quad (3)$$

and

$$S_T(k) = \beta \epsilon^{-1/3} \chi k^{-5/3} \quad (4)$$

where  $\alpha$  and  $\beta$  are constants equal to .25 and .8 respectively. The latter expression was formulated by Corrsin (1951).

This paper describes results from a comparison of a very substantial amount of  $C_T^2$  data obtained over the open ocean with the Wyngaard et al. (1971) predictions based on bulk surface layer measurements. Friehe (1976) performed a similar comparison in which fewer data were used and in which a different bulk stability parameter was used. He concluded that reasonable prediction of  $C_T^2$  could be made from bulk formulations.

## 2. Surface Layer Bulk Aerodynamic Relations for $C_T^2$

Wyngaard, et al. (1971) related  $C_T^2$  to surface fluxes with Eq. 2 using separate expressions for  $\epsilon$  and  $\chi$  based on overland measurements. The general expression was

$$\frac{C_T^2 Z^{2/3}}{T_*^2} = f(\xi); \quad \xi = \frac{Z}{L} \quad (5a)$$



$$\text{where} \quad f(\xi) = \begin{array}{ll} 4.9(1 - 7\xi)^{-2/3} & \xi < 0 \\ 4.9(1 + 2.4 \xi^{2/3}) & \xi > 0 \end{array} \quad \begin{array}{l} (5b) \\ (5c) \end{array}$$

It is noted that these interpolation formulae still lack substantial verification for the overwater regime.

These formulae agree with the expected asymptotic scaling (Wynngaard, 1973) for  $C_T^2$  under very unstable (local free convection) and very stable (Z-less) stratifications. The appropriate scaling formulations in the extreme stability limits are

$$\text{free convection:} \quad \frac{C_T^2 Z^{2/3}}{T_f^2} = \text{constant} \quad (6)$$

$$\text{where} \quad T_f = (TQ_o^2/gZ)^{1/3}; \quad Q_o = \overline{w'\theta'}$$

$$\text{Z-less:} \quad \frac{C_T^2 L^{2/3}}{T_*^2} = \text{constant} \quad (7)$$

Therefore, the asymptotic predictions are for  $C_T^2$  to vary as  $Z^{-4/3}$  for free convection and to be independent of height (Z-less) for very stable conditions.

In this study, boundary flux parameters in Eq. 5, ( $T_*$  and  $L$ ) were calculated using bulk aerodynamic formulae. Bulk aerodynamic formulae are those which relate boundary scaling parameters to the wind speed at a level and the temperature and humidity difference between that level and the surface. Their use for indirect estimates of the boundary fluxes has received considerable attention in overwater observational experiments because of difficulties in making eddy flux, and profile measurements.

The bulk aerodynamic formulae at a height Z for the velocity and potential temperature scaling parameters are:

$$u_* = C_D^{\frac{1}{2}} U \quad (8)$$

$$T_* = C_\theta^{\frac{1}{2}} (\theta_Z - \theta_S) \quad (9)$$

where S refers to the surface value and  $C_D$  and  $C_\theta$  are drag coefficients. The drag coefficients depend upon height, stability, and wind velocity. Similarly, for the sensible heat flux

$$-\overline{w'\theta'} = C_H U (\theta_Z - \theta_S) \quad (10)$$

where

$$C_H = (C_D C_\theta)^{\frac{1}{2}} \quad (11)$$

Since several publications give detailed descriptions of the bulk method with various experimental values for the drag coefficients, we shall restrict this discussion to a few points that must be considered when relating overwater measured values of  $C_T^2$  to values of  $T_*$  and  $\xi$  based on bulk method calculations. In particular, we must note that  $T_*$  is directly dependent upon the value of  $C_\theta^{\frac{1}{2}}$  (Eq. 9). Using conventions developed by Liu (1978), the neutral stability temperature drag coefficient is given by (in this convention,  $(\alpha_{TK} Z/T_*)(\partial\theta/\partial Z)$  is the dimensionless profile function)

$$C_{\theta N}^{\frac{1}{2}} = \alpha_{TK} [\ln(Z/Z_{OT})]^{-1} \quad (12)$$

where  $\kappa$  is von Karman's constant,  $\alpha_T$  the ratio of heat and momentum transport diffusivities (at neutral stability) and  $Z_{OT}$  is the appropriate roughness length for the temperature profile. Since Wyngaard, et al.'s expression for  $f(\xi)$  was based upon direct measurement of  $T_*$  from the heat flux and Reynold's stress, their curve was not dependent upon a choice of  $C_{\theta N}$ . In view of this, we will select the value of  $C_{\theta N}$  that yields the best fit to our data, treating this as an indirect measurement of  $C_{\theta N}$ .

The dependence of overwater neutral momentum drag coefficients,  $C_{DN}$ , on wind speed has been the objective of many investigations. For our analyses, we chose a recently suggested representation by Kondo (1975), Table 1.

The stability dependence of  $C_D$  and  $C_\theta$  is defined on the basis of the following general expressions

$$C_D = \frac{C_{DN}}{[1 - (\kappa)^{-1} C_{DN}^{\frac{1}{2}} \psi_1(\xi)]^2} \quad (13)$$

$$C_\theta = \frac{C_{\theta N}}{[1 - (\alpha_T \kappa)^{-1} C_{\theta N}^{\frac{1}{2}} \psi_2(\xi)]^2} \quad (14)$$

where  $\psi_1(\xi)$  and  $\psi_2(\xi)$  are stability corrections to wind and scalar profiles. Formulations for  $\psi_1(\xi)$  and  $\psi_2(\xi)$  have been presented by Businger (1973) and ours were similar except for the use of  $\alpha_T$  normalization (Liu, 1978).

The dependence of the drag coefficients on stability leads to computational considerations in estimating  $\xi$  since the coefficients which define the latter are themselves functions

of  $\xi$  as indicated by the following bulk expression

$$\xi = \xi_0 \left[ \frac{(1 - \kappa^{-1} C_{DN}^{\frac{1}{2}} \psi_1(\xi))^2}{(1 - (\alpha_T \kappa)^{-1} C_{\theta N}^{\frac{1}{2}} \psi_2(\xi))} \right] \quad (15)$$

where

$$\xi_0 = \kappa \frac{gZ}{T} \frac{C_{\theta N}^{\frac{1}{2}}}{C_{DN}} \left[ \frac{\Delta\theta + .18\Delta Q}{U^2} \right] \quad (16)$$

All parameters are in the MKS units with  $Q$  in gm/kg.

$\xi_0$  is the equivalent of a first guess of  $\xi$  based on bulk differences and neutral values for the drag coefficients. For each value of wind velocity, we calculated  $C_{DN}$ , allowing calculation of  $\xi_0$ . The final value of  $\xi$  was found by solving Eq. 15, iteratively. An example set of solutions is shown in Fig. 1 for  $U = 7.6$  m/sec.

Friehe (1976) effectively defined  $\xi$  as being equal to  $\xi_0$  when he compared overwater  $C_T^2$  values with bulk parameter predictions based on Eq. 5. He used a constant  $C_{DN}$  value and two different values of  $C_{\theta N}$ , depending on the value of  $U\Delta\theta$ . The differences between the solid curve and dashed lines in Fig. 1 represent the difference which would arise in neglecting stability effects in the specification of  $\xi$ .

### 3. Experimental Arrangements

The data were obtained during several experiments conducted during a four year period (1974-1978), over an extensive ocean area and aboard three different ships (listed in Table 2). The instrumentation was designed for profile measurements of both mean and turbulent parameters. In all experiments, these were made at multi-levels on two masts separated spatially on the



forward part of the ships (Fig. 2). A comprehensive description of the system is the subject of another paper (Houlihan, et al., 1978).

Mean temperature was measured with quartz oscillator thermometers, accurate to  $.01^{\circ}\text{C}$ . Mean humidity was measured with Li Cl sensors, accurate to about 3%RH. Wind velocity was measured with cup anemometers, accurate to about 5%. Temperature fluctuations (for  $C_T^2$ ) were measured with ac Wheatstone bridges (3.0 KHz carrier), using paired resistance probes with  $2.5\mu\text{m}$  diameter platinum wires. The resistance probes were mounted on wind vanes to maintain correct alignment with the relative wind direction.

Two features of the measurement arrangement significant in the interpretation of results are the aspiration of mean temperature sensors and the surface temperature measurements. The quartz temperature sensors and humidity sensors were contained within aspirated weather shelters. The shelters had two purposes: to protect the sensors from the marine environment and to reduce radiation effects. Radiation effects were of special concern, since some of the sensors were above the water and some were above the deck of the ships, which are heated by the sun and radiate strongly. Because of radiation from the deck, we modified the shelters, placing a shield at the base of the unit to reduce radiation from below. Even with these precautions, systematic temperature corrections for the aspirators (during day and night operations) have been determined from calibrations with a glass dewar type aspirator. The daytime correction  $.6^{\circ}\text{C}$  and the nighttime correction is  $.4^{\circ}\text{C}$  (subtracted from measured temperature).

The sea surface temperature sensor (a quartz probe) was attached to a plastic hose so that it floated within one inch of the surface. On all ships, its location was aft of the midship. The location on all of these ships, underway and holding position, was definitely influenced by the ship's wake.

The mean data were continuously averaged and periodically logged by a microprocessor developed at the Naval Postgraduate School and adopted for the R/V ACANIA by Plunkett (1977). Mean values were defined for 15 to 30 minute periods. Most periods were 30 minutes long, the planned duration, but shorter periods occurred due to such events as change in the ship's course.

#### 4. Data Evaluation and Error Analysis

Comparison of  $C_T^2$  results and available expressions are made with  $T_*$  and  $L$  values estimated from 10 meter wind, temperature, and humidity and surface temperature values. Initial plans were also to estimate  $T_*$  and  $L$  values from mean profile data, as evident from previously described instrumentation arrangements. The latter results are not presented because of inconsistencies which have been attributed to difficulties in defining small scalar and wind gradients. Although these same errors existed in the mean data used for bulk estimates, the accuracy requirements of the bulk method are much less stringent.

The 10 meter mean, as well as  $C_T^2$  values, were obtained by interpolating from levels above and below, if available, or by extrapolating on the basis of expected height variations, if only one level was available. With these specifications,  $T_*$  and  $\xi$  were computed for the 10 meter level, using Eqs. 9 and 15.

Two aspects of the measurements require further discussion for this study. These are the influence of salt contamination on resistance wire sensors, and uncertainties in the surface temperature specification. Although the latter may not be significant for some applications, it is significant in our results, because the air-surface temperature difference occurs as a squared quantity in scaling  $C_T^2$  by  $T_*^2$ .

The influence of salt contamination of resistance wires and thermocouples, and hence, all temperature fluctuation measurements in the marine environment, was recently described by Schmitt, et al. (1978). These effects were discussed by Friehe (1977) in his comparison between overwater  $C_T^2$  values and bulk aerodynamic predictions and led him to limit the data considered. Schmitt, et al. (1978) suggested that erroneous temperature fluctuations occur due to water vapor absorption and evaporation on the salt nuclei attached to the wire. This occurs in conjunction with fluctuations in ambient RH. The effect is manifested by the occurrence of spikes in the temperature trace. These spikes can cause overwater temperature variance spectra to exhibit non-Kolmogorov slopes.



In an effort to eliminate the salt effect, the resistance wires were washed or changed at frequent intervals during the latest experiment (CEWCOM-78). Mean ratios of  $C_T^2$  immediately before and after washing versus relative humidity appear in Fig. 3. We observed that  $C_T^2$  values from contaminated wires are larger for an RH range from 50% to 85%, only. Presumably, the effect is diminished at RH above 85% because humidity fluctuations are less intense due to the small RH gradient. Their effect, as described, is within the system accuracy. Presumably, the effect is diminished at RH below 50% because the salt nuclei attached to the wires are not activated, hence, humidity fluctuations do not cause significant absorption or evaporation.

We tested these interpretations by computing the ratio of measured  $C_T^2$  to computed  $C_T^2$  (using Eq. 5 and bulk parameter estimates of  $T_*$  and  $\xi$ ) with data from all experiments except CEWCOM-78. Mean values of these ratios versus RH appear in Fig. 4. The individual points are mean values for 5% RH intervals and the error bars are expected errors of the averages ( $\pm \sigma/\sqrt{N}$ ,  $N$  = number of points) within each interval. The number at the top of the error bar is  $N$ . These data exhibit values near 1 for RH values above 85%. There are slight increases at 95% and at 85% and there is a significant increase at 80%. The ratios are larger at low RH values, compared to corresponding result from clean wires in CEWCOM-78.

Differences between the results in Fig. 3 (washing and replacement) and the results in Fig. 4 (from the other experiments) are the larger values of the ratio at very low RH values and the

lower values above 95%. The former result is not unexpected, because wires exposed for longer periods without cleaning as they were for the other experiments would be sufficiently contaminated to respond to large humidity fluctuations, even if they were not activated. The latter result could also be attributed to the degree of contamination and the tendency of salt particles to grow into water droplets at high RH. Contaminated wires at large RH values experience a loss of frequency response, resulting in a lower sensitivity to temperature fluctuations.

Based on the above results, we decided to consider only those  $C_T^2$  data measured at RH values above 82.5%.  $C_T^2$  results obtained with lower RH values were excluded except from periods immediately following sensor replacement. All data from CEWCOM-78 which were from clean sensors were considered.

We used intermediate  $C_T^2$  and  $\Delta\theta$  results to examine uncertainties in the sea surface temperature. These results appear in Fig. 5 where  $C_T^2$  data were selected on the basis of RH considerations and  $\Delta\theta$  values have been adjusted for systematic aspirator corrections. If the measured surface temperatures were the "skin" temperatures, we expect the minimum in  $C_T^2$  to occur near  $\Delta\theta$  equal to zero. This is the case for both night and day. However, we estimate that our  $\Delta\theta$  values are subject to uncertainties as large as  $.5^\circ\text{C}$ , based on the displacement and broadness of the daytime  $C_T^2$  minimum. This is primarily due to an inability to ensure that the sea surface sensor actually measured the skin temperature. Liu (1978)

suggests how the latter problem could have been treated with interface flux equilibrium considerations. However, his suggested procedures were not applied to these data because they apply to a bucket temperature which was not measured by our sensor.

The results of an analysis of measurement errors appear in Table 3. These are the errors introduced by instrument accuracies, noise and uncertainties in certain calibration values. In the case of  $C_T^2$ , most of the uncertainty is due to the salt contamination effect. In the case of  $T_S$ , the sensor itself is accurate to  $.01^\circ\text{C}$ , but one cannot be certain that the sensor is in fact measuring the surface temperature.

## 5. Results

Dimensionless temperature structure parameter (DTSP) versus  $\xi$  results appear in Fig. 6, in the format used by Wyngaard, et al. (1971). Again, error bars are the uncertainties of the means and the numbers are the number of points defining the mean. For this comparison,  $C_{\theta N}$  was determined by assuming that  $Z_{OT}$  was independent of velocity and had a value corresponding to  $Z_o$  for a typical drag coefficient,  $C_{DN} = 1.3 \times 10^{-3}$ . The appropriate value of  $C_{\theta N}$  for a measured  $C_T^2$  was estimated from the following equation,

$$C_{\theta N} = \left( \frac{C_T^2 Z^{2/3}}{f(\xi)} \right) \frac{[1 - (\ln Z/Z_{OT})^{-1} \psi_2(\xi)]^2}{\Delta\theta^2} \quad (17)$$

The value of  $C_{\theta N}$  selected was that from the CEWCOM-78 data, since these were least influenced by salt contamination.

Although it was necessary to assume an initial value of  $C_{\theta N}$  to obtain the values of  $\xi$ , the final results (Fig. 7)

are fairly insensitive to the initial choice. A minimum  $|\xi|$  value of .05 was used in this determination in view of the uncertainties listed in Table 3. The value of  $C_{\theta N}$  selected and, hence, used to compute  $T_*$  and  $\xi$  for the results in Fig. 6 was  $1.3 \times 10^{-3}$ . Using  $C_{HN} = (C_{DN} C_{\theta N})^{\frac{1}{2}}$ , we compare this  $C_{\theta N}$  value with some obtained from measurements of  $C_{HN}$  (Table 4), assuming a typical  $C_{DN}$  value of  $1.3 \times 10^{-3}$  if not given.

DTSP results are also presented with logarithmic  $\xi$  axes, Fig. 8. This format enables examination of the distributions of the large number of results near  $\xi$  equal to zero in a more illustrative perspective. Also, results at  $\xi$  values less than -7 which were not included in Fig. 6, can now be viewed.

This format demonstrates the exceptional agreement between the results and the prediction over the range,  $-.03 < \xi < -7$ . Also, disagreement between observed and predicted results can be readily related to previously mentioned measurement uncertainties. Disagreements at the minimum  $|\xi|$  intervals, for both stable and unstable sides, are attributed to errors in specifying  $\Delta\theta$  as well as inherent noise in the  $C_T^2$  measurement and recording systems. Disagreement at large  $|\xi|$  values on the unstable side is attributed to increased  $C_T^2$  values due to the salt contamination effect, since these data happen to have corresponding relative humidity values near 85%.

DTSP results based on asymptotic scaling for unstable (Eq. 6, free convection) and stable (Eq. 7, Z-less) conditions appear in Figs. 9a and 9b, respectively. Predictions based on



Eq. 5 (a and b) appear as solid curves. For the unstable side, the prediction was approximated as

$$\frac{C_T^2 Z^{2/3}}{T_f^2} = 9.9 \frac{|\xi|}{1-7\xi}^{2/3} \quad (18)$$

which approaches a value of 2.7 for large  $|\xi|$ . Eq. 18 is not correct when  $q_*$ , as well as  $T_*$ , determines  $\xi$ . When  $q_*$  is negative (typical marine conditions), the observed values should be less than predicted by this expression. This is the case for these results. For the stable side, the prediction is

$$\frac{C_T^2 L^{2/3}}{T_*^2} = 4.9 [\xi^{-2/3} + 2.4] \quad (19)$$

which approaches a value of 11.8 for large  $\xi$ .

In summary, the DTSP results agree very well with the predictions under unstable conditions and reasonably well under stable conditions. Under stable conditions, they are slightly less than the predictions. The determined  $C_{\theta N}$  value agrees reasonably well with those reported. DTSP disagreement under neutral conditions ( $|\xi| < .05$ ) is attributed to uncertainties in measuring the air-sea temperature difference and inherent system and measurement noise. The latter would include the salt contamination effect, since any humidity fluctuation would cause apparent temperature fluctuations. Disagreement under very unstable conditions,  $\xi < -7$ , was due to the fact that these data occurred with

RH values,  $\approx 85\%$ , not totally immune to the salt contamination effect.

The actual significance of the slight disagreement under stable conditions is somewhat uncertain. However, it could also be attributed to the salt contamination effect. During stable conditions over the ocean, humidity and temperature fluctuations are negatively correlated. Hence, dry-warm or moist-cold eddies are causing the fluctuations. In the case of dry-warm parcels, contaminated sensors would be experiencing a cooling due to evaporation, but a compensating heating due to the temperature change would also occur. In the case of cold-moist parcels, the reverse would occur.

DTSP results based on asymptotic scaling appeared to approach the predicted constants at the limits. Agreement for these results was expected, on the basis of agreement in other DTSP results, because Monin-Obukhov scaling was used in determining  $T_f$ . This arose when  $Q_0$ , in Eq. 6, was determined from  $T_*$  and  $U_*$  values which were estimated on the basis of Monin-Obukhov scaling.

The multi-level  $C_T^2$  data enabled an examination of predicted height variation, under different stability conditions. These results appear in Fig. 10 where A is the coefficient obtained for the best fit linear relation between observed  $\text{Log } C_T^2$  values and  $\text{Log } Z$  values,

$$\text{Log } C_T^2 = A \text{ Log } Z + B. \quad (20)$$

The curves are predictions obtained by determining  $d\log C_T^2/d\log Z$  from Eq. 5 and approach limiting values of  $-4/3$  and  $0$  on the unstable and stable sides and a value of  $-2/3$  at the neutral point.

Fewer periods were available for this examination than for the preceding  $C_T^2$  results. This was because probes at upper levels, which were not readily accessible, were not always replaced when they became inoperative. Also, we measured  $C_T^2$  at a single level during CEWCOM-78 because of frequent probe washing and replacement.

Results in Fig. 10 indicate that height dependence of observed  $C_T^2$  values agreed quite well with the prediction. This is particularly the case for the stability variation of the dependence. A majority of the mean values indicate that  $C_T^2$  decreased somewhat less rapidly with height than the prediction. This result could be attributed to system noise which contributed the same at all levels and would reduce the apparent relative difference (decrease) between levels. Evidence for this is the larger (relative) disagreement at near neutral (unstable) intervals, where the signal to noise ratio is the smallest.

## 6. Conclusions

Comparisons of a substantial amount of overwater  $C_T^2$  data have been made with predictions of the existing empirical expressions. Measured overwater  $C_T^2$  data, which were selected to minimize the salt contamination influence are described



very well by Wyngaard, et al's (1971) expressions, even with bulk surface flux estimates. An estimated  $C_{0N}$  value of  $1.3 \times 10^{-3}$  agrees with lower values obtained by others. Disagreements exceeding measurement accuracies (20-30%) occur for near neutral conditions where  $C_T^2$  is insignificant in most applications, and for large unstable conditions. These disagreements are attributed to measurement difficulties rather than to the validity of the existing expressions. Agreement between observed and predicted height distributions over the full stability range provide further verification of the existing expression.

In conclusion, a typical (but not the best) comparison of observed and predicted  $C_T^2$  values during a 24 hour period in CEWCOM-78 is presented in Fig. 11a to further demonstrate the overwater applicability of the expressions. The predicted values based on bulk estimates of surface fluxes are within the accuracy of the measurements in describing the observed values. Coincident bulk  $|\xi|$  estimates for the period appear in Fig. 11b.

#### ACKNOWLEDGEMENTS

Work supported by the following commands of the U. S. Navy: Oceanographer of the Navy (Code 3100), Naval Sea Systems Command (PMS 405), and Naval Air Systems Command (AIR 370).

We wish to acknowledge the contributions of Ray Garcia, Lyn May, Steven Rinard, Jeffrey Haltiner, Charles Leonard, Vicki Culley, and Captain Reynolds and the crew of the R/V ACANIA.

## REFERENCES

- Businger, J. A. (1973): "Turbulent Transfer in the Atmospheric Surface Layer," Chapter 2, Workshop on Micrometeorology, D. Harugen, Editor, American Meteorological Society, 67-98.
- Champagne, F. H., Friehe, C. A., LaRue, J. C., and Wyngaard, J. C., (1977): "Flux Measurements, Flux Estimation Techniques and Fine-Scale Turbulence Measurements in the Unstable Surface Layer Over Land." J. Atmos. Sci., 34, 513-530.
- Corrsin, S. (1951): "On the Spectrum of Isotropic Temperature Fluctuations in an Isotropic Turbulence," J. Appl. Phys., 22, 469-473.
- Davidson, K. L. (1974): "Observational Results on the Influence of Stability and Wind-Wave Coupling on Momentum Transfer and Turbulent Fluctuations over Ocean Waves, Boundary Layer Meteorology, 6, 305-331.
- Dunckel, M., Hasse, L., Krugermeyer, L., Schriever, D., and Wucknitz, J., (1974): "Turbulent Fluxes of Momentum, Heat and Water Vapor in the Atmosphere Surface Layer at Sea During ATEX, Boundary Layer Meteorol., 6, 81-106.
- Friehe, C. A. (1976): "Estimation of the Refractive-Index Temperature Structure Parameter in the Atmospheric Boundary Layer over the Ocean," Applied Optics, 16, 334-340.
- Friehe, C. A., LaRue, J. C., Champagne, F. H., Gibson, C. H., and Dreyer, G. F. (1975): "Effects of Temperature and Humidity Fluctuations on the Optical Refractive Index in the Marine Boundary Layer." J. Opt. Soc. Amer., 65, 1502-1511.
- Friehe, C. A. and Schmitt, K. F., (1976): "Parameterization of Air-Sea Interface Fluxes of Sensible Heat and Moisture by the Bulk Aerodynamic Formulas," J. Phys. Oceanogr., 6, 801-809.
- Houlihan, T. M., Davidson, K. L., Fairall, C. W., and Schacher, G. E., (1978): "Experimental Aspects of a Shipboard System Used in Investigation of Overwater Turbulence and Profile Relationships," I.E.E.E., J. of Oceanogr. Instr. (submitted).
- Kondo, J. (1975): "Air-Sea Bulk Transfer Coefficients in Diabatic Conditions," Boundary Layer Meteorology, 9, 91-112.
- Liu, W. T. (1978): "The Molecular Effects on Air-Sea Exchanges," Ph.D. Dissertation, University of Washington, Seattle, WA, 170 pp.
- Muller-Glewe, J. and Hinzpeter, H., (1974): "Measurement of the Turbulent Heat Flux Over the Sea," Boundary Layer Meteorol., 6, 47-52.
- Plunkett, J. R. (1976): "A Microprogrammable Data Acquisition and Control System (MIDAS II A) with Application to Mean Meteorological data," M. S. Thesis, Naval Postgraduate School, Monterey, CA 144 pp.

- Pond, S., Fissel, D. B., and Paulson, C. A. (1974): "A Note on Bulk Aerodynamic Coefficients for Sensible Heat and Moisture Fluxes," Boundary Layer Meteorol., 6, 333-340.
- Schmitt, K. F., Friehe, C. A., and Gibson C. H. (1978): "Humidity Sensitivity of Atmospheric Temperature Sensors by Salt Contamination," J. Phys. Oceanogr., 8, 115-161.
- Smith, S. D., (1974): "Eddy Flux Measurements over Lake Ontario," Boundary Layer Meteor., 6, 235-256.
- Wyngaard, J. C. (1973): "On Surface-Layer Turbulence," Chapter 3, Workshop on Micrometeorology, D. Haugen, Editor, American Meteorological Society, 101-149.
- Wyngaard, J. C., Izumi, Y., and Collins, S. A., (1971): "Behavior of the Refractive Index Structure Parameter near the Ground," J. Opt. Soc. Am., 61, 1646-1650.

## LIST OF TABLES

- Table 1.  $C_{DN}$  versus wind speed (10 meter) from Kondo (1975).
- Table 2. Summary of Experiments
- Table 3. Error analysis for measured, intermediate, and scaling parameters
- Table 4. Empirically determined sensible heat drag coefficients,  
 $\times 10^3$

Table 1.  $C_{DN}$  versus wind speed (10 meter)  
from Kondo (1975).

$\underline{U \text{ ms}^{-1}}$	$\underline{C_{DN} \times 10^3}$
.3 - 2.2	$1.08 \times U^{-.15}$
2.2 - 5.0	$.77 + .086 \times U$
5.0 - 8.0	$.87 + .067 \times U$
8.0 - 25.0	$1.2 + .025 \times U$



TABLE 2. Summary of Experiments

<u>EXPERIMENT</u>	<u>SHIP</u>	<u>LOCATION</u>	<u>PERIOD</u>	<u>NUMBER OF PERIODS</u>
	R/V ACANIA <sup>4</sup>	Monterey Bay	All Months 1973-76	98
CEWCOM-76 <sup>1</sup>	R/V ACANIA	E. Pacific	Sep-Oct 76	285
NRL - EOMET <sup>2</sup>	USNS HAYES <sup>5</sup>	N. Atlantic & Mediterranean	May-Jun 77	269
	USNS KANE <sup>6</sup>	Mid-Atlantic	Feb-Mar 78	38
CEWCOM-78 <sup>3</sup>	R/V ACANIA	E. Pacific	May 1978	200
			Total	890

<sup>1</sup>Cooperative Experiment West Coast Oceanography & Meteorology-1976

<sup>2</sup>Naval Research Laboratories, Electro-Optical Meteorology Cruise

<sup>3</sup>Cooperative Experiment West Coast Oceanography & Meteorology-1978

<sup>4</sup>Operated by Department of Oceanography, Naval Postgraduate School, Monterey, California

<sup>5</sup>Operated by Naval Research Laboratories, Washington, D. C.

<sup>6</sup>Operated by Naval Oceanographic Office, Washington, D. C.

Table 3. Error analysis for measured,  
intermediate, and scaling parameters

Measured	$T_S$	$T_Z$	U	RH	$C_T^2$
RMS Error ( $\pm$ )	.3°C	.2°C	8%	3%	30%
Intermediate	$\Delta\theta$		$\Delta Q$		
Accuracy ( $\pm$ )	.5°C		.4 gm/Kg		
Scaling	$U_*$	$T_*$	$Q_*$	$\xi$	
Accuracy ( $\pm$ )	10%	.02°C	.02 gm/Kg	.03 or 30%	



Table 4. Empirically determined sensible  
heat drag coefficients,  
 $\times 10^3$

<u>Sources</u>	$C_{HN}$	$C_{DN}$	$C_{\theta N}$
Pond, et al. (1974)	1.5	1.45	1.55
Dunckel, et al. (1974)	1.5	1.60	1.40
Muller-Glewe and Hinzpeter (1974)	1.0	(1.30) <sup>1</sup>	.77
Smith (1974)	1.2	1.02	1.41
Friehe and Schmitt (1976)	.91 <sup>2</sup>	(1.30)	.64
This study	1.3	1.30	1.34

<sup>1</sup>( ) denotes assumed  $C_N$  value; other given by authors

<sup>2</sup>Excludes high wind data

- Figure 1. Ratio of  $\xi$  based on stability dependent drag coefficients ( $\xi$ ) to  $\xi$  based on constant drag coefficients ( $\xi_0$ ) versus  $\xi_0$ .
- Figure 2. Schematics of shipboard mounting arrangements. (a) R/V ACANIA, (b) USNS HAYES, and (c) USNS KANE.
- Figure 3. Ratio of  $C_T^2$  (before to after replacement or washing) versus RH; (From CEWCOM-78).
- Figure 4. Ratio of measured  $C_T^2$  to computed  $C_T^2$  (from Eq. 5) versus RH, for all except CEWCOM-78 data.
- Figure 5.  $C_T^2$  versus  $\Delta\theta$  (a) daytime (0800-1900 LST), (b) nighttime (1900-0800 LST).
- Figure 6. Mean DTSP versus  $\xi$  results. Solid curve is prediction based on Eq. 5.
- Figure 7.  $C_{\theta N}$  versus  $\xi$  results.  $C_{\theta N}$  based on Eq. 17 and CEWCOM-78 results.
- Figure 8. Same as Figure 6 with logarithmic  $\xi$  axis.
- Figure 9. DTSP based on asymptotic scaling. (a) free convection curve is approximate prediction, Eq. 18 and, (b) Z-less, curve is prediction, Eq. 19.
- Figure 10. Height variations of  $C_T^2$  versus  $\xi$ .  $A(C_T^2)$  is defined by Eq. 20, solid curves are prediction based on Eq. 5.
- Figure 11. Results from 24 hour period during CEWCOM-78 (a) Observed and Predicted  $C_T^2$  for 10 meters (b) Observed  $\xi$ .

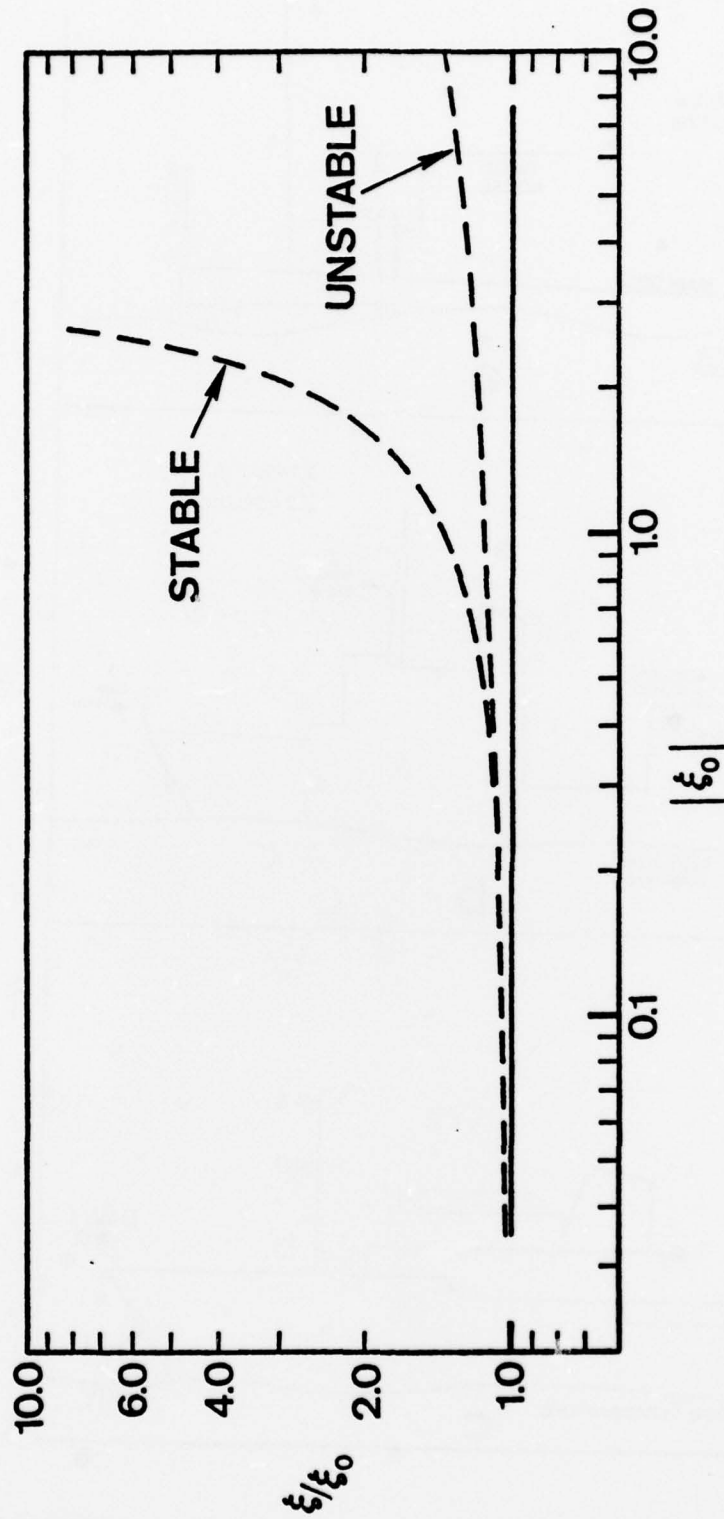


Figure 1. Ratio of  $\xi$  based on stability dependent drag coefficients ( $\xi$ ) to  $\xi$  based on constant drag coefficients ( $\xi_0$ ) versus  $\xi_0$ .

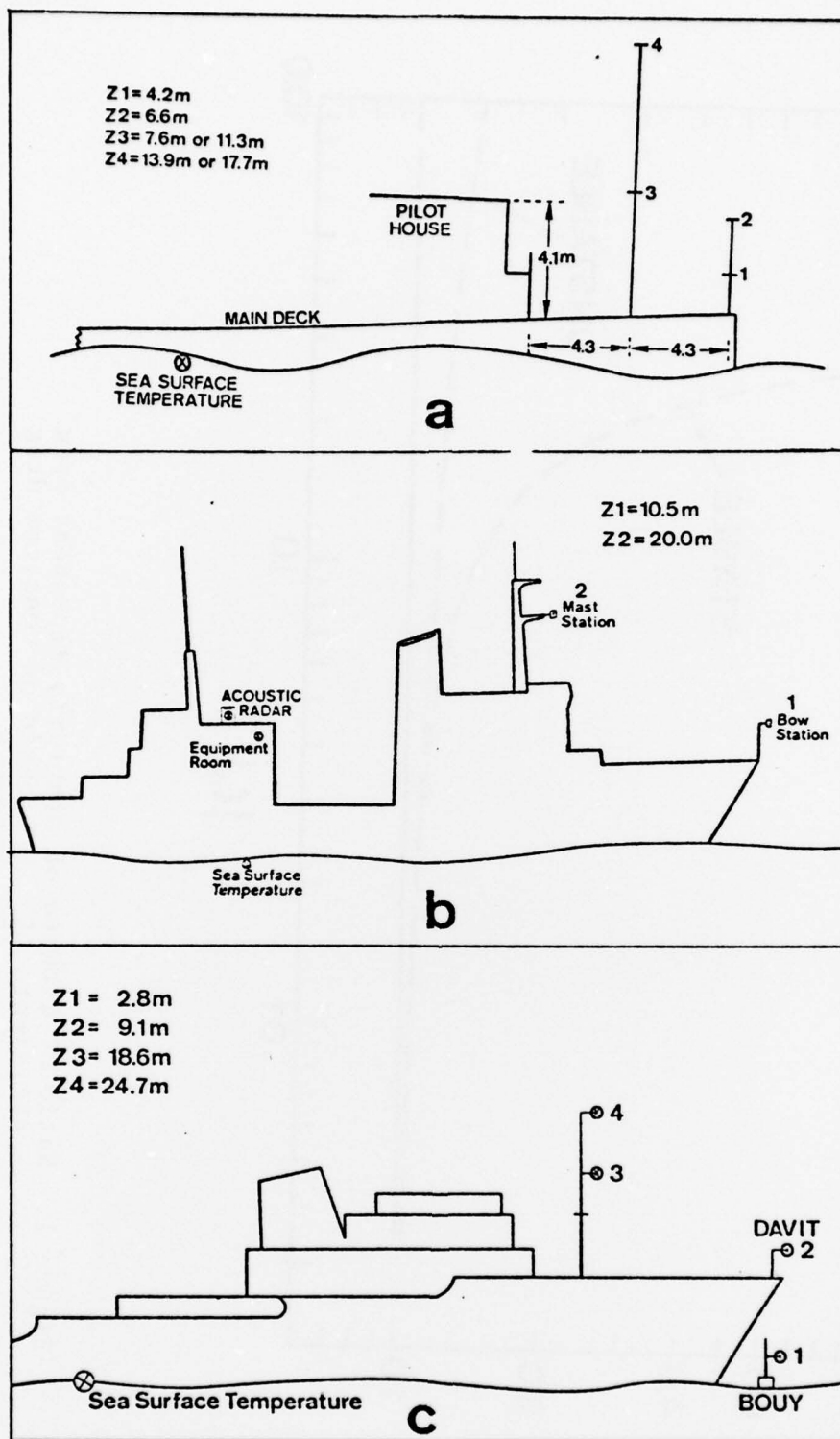


Figure 2. Schematics of shipboard mounting arrangements, (a) R/V ACANIA, (b) USNS HAYES, and (c) USNS KANE.

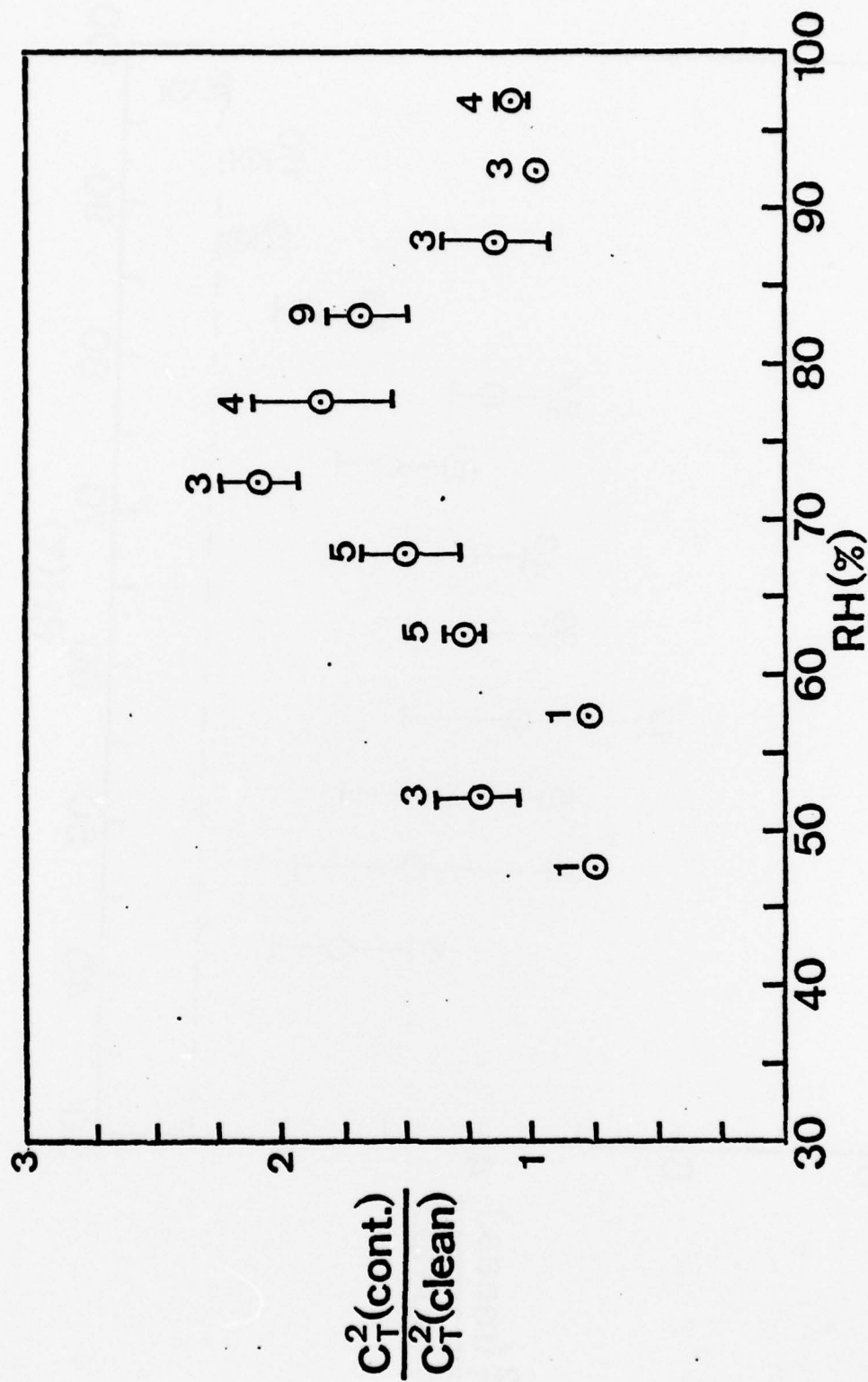


Figure 3. Ratio of  $C_T^2$  (before to after replacement or washing) versus RH; (From CEWCOM-78).



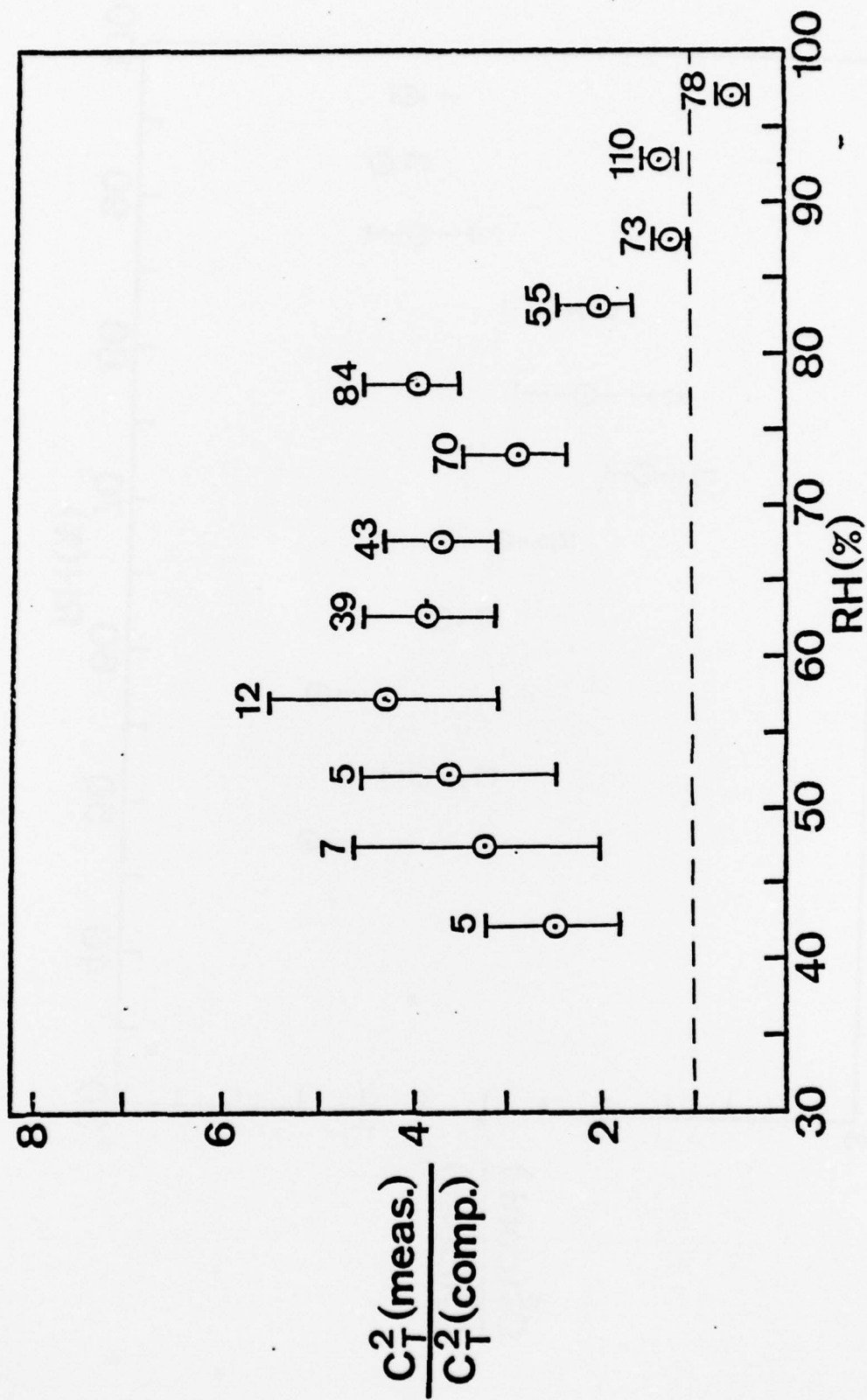


Figure 4. Ratio of measured  $C_T^2$  to computed  $C_T^2$  (from Eq. 5) versus RH, for all except CEWCOM-78 data.

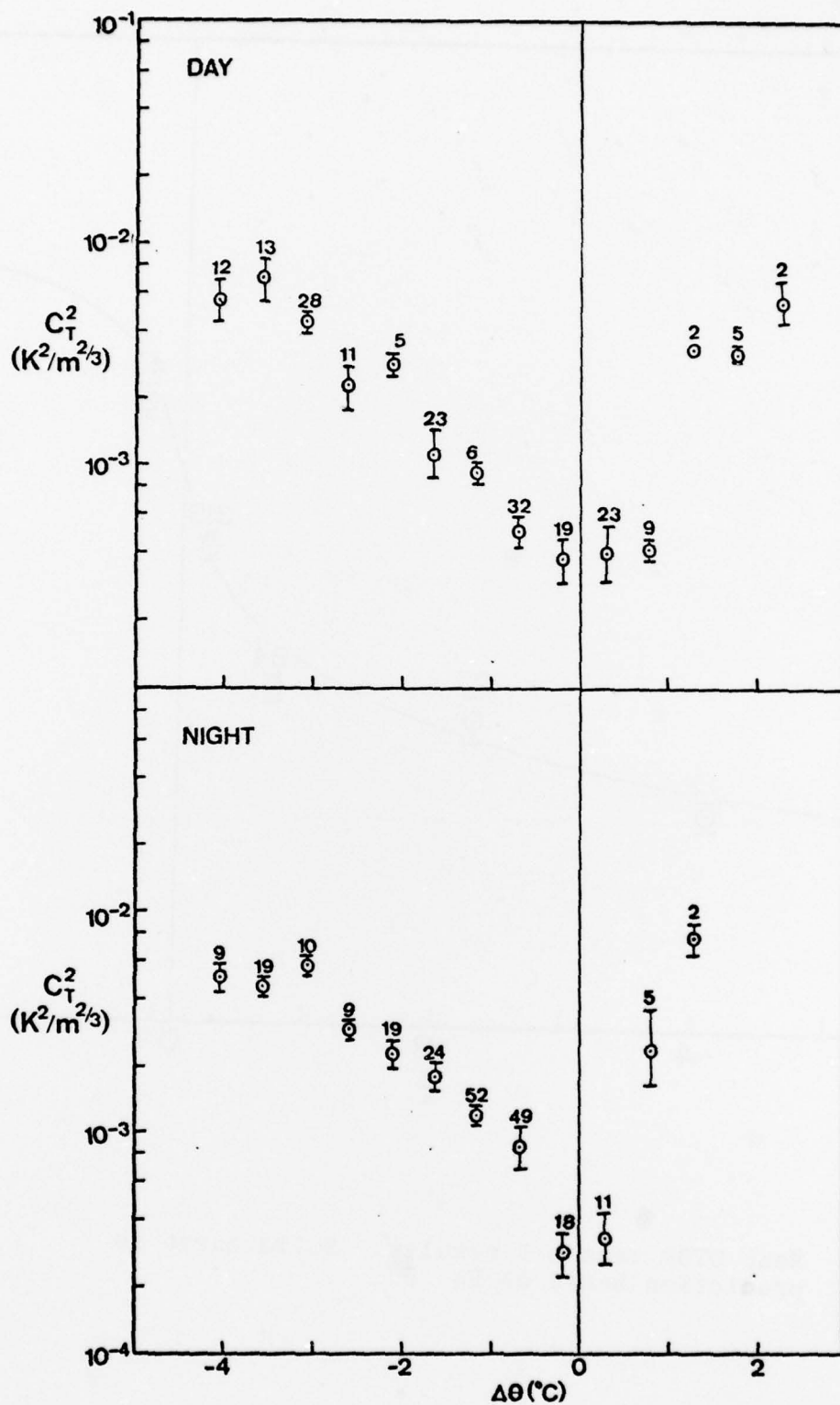


Figure 5.  $C_T^2$  versus  $\Delta\theta$  (a) daytime (0800-1900 LST),  
(b) nighttime (1900-0800 LST).

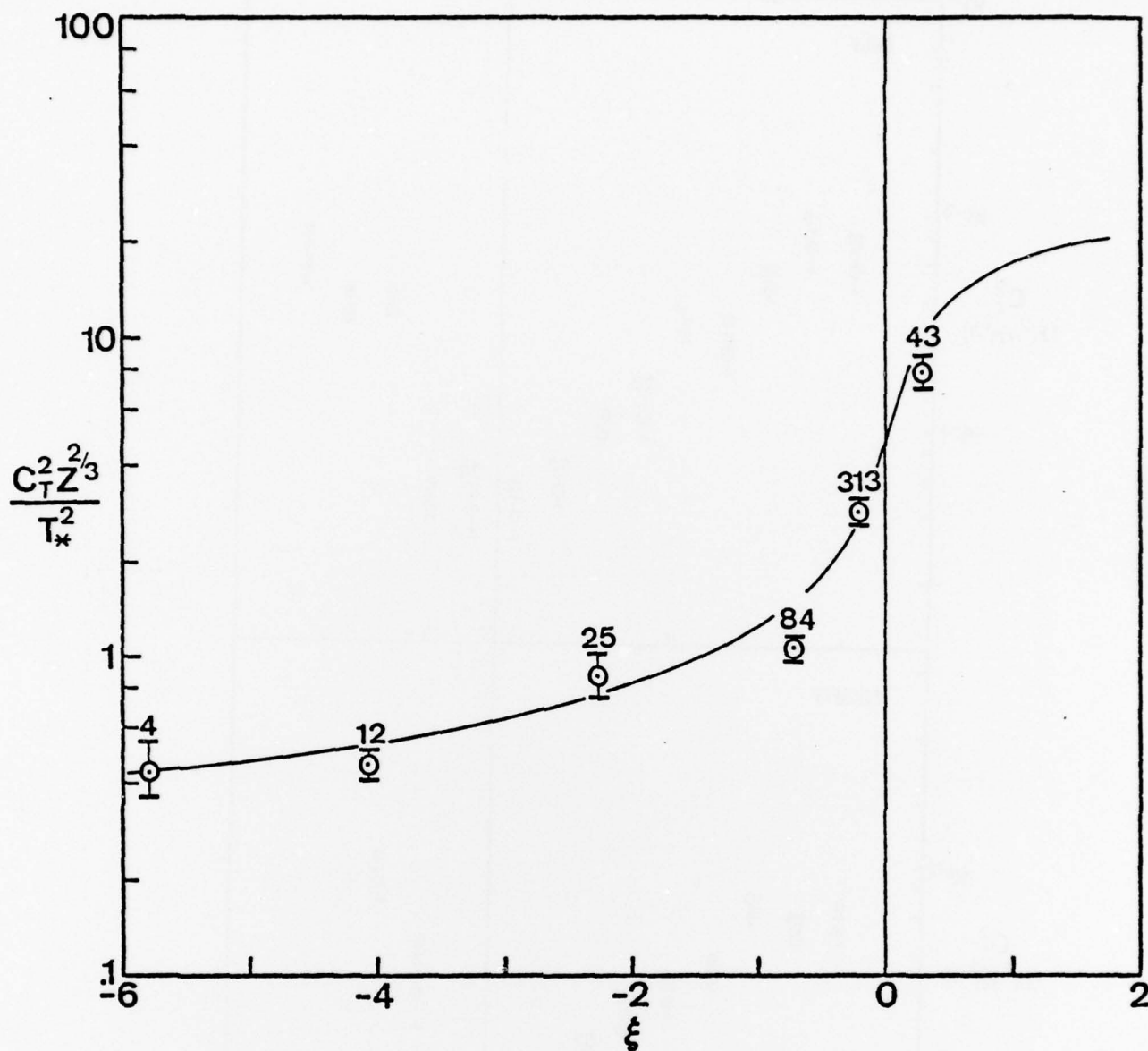


Figure 6. Mean DTSP versus  $\xi$  results. Solid curve is prediction based on Eq. 5.

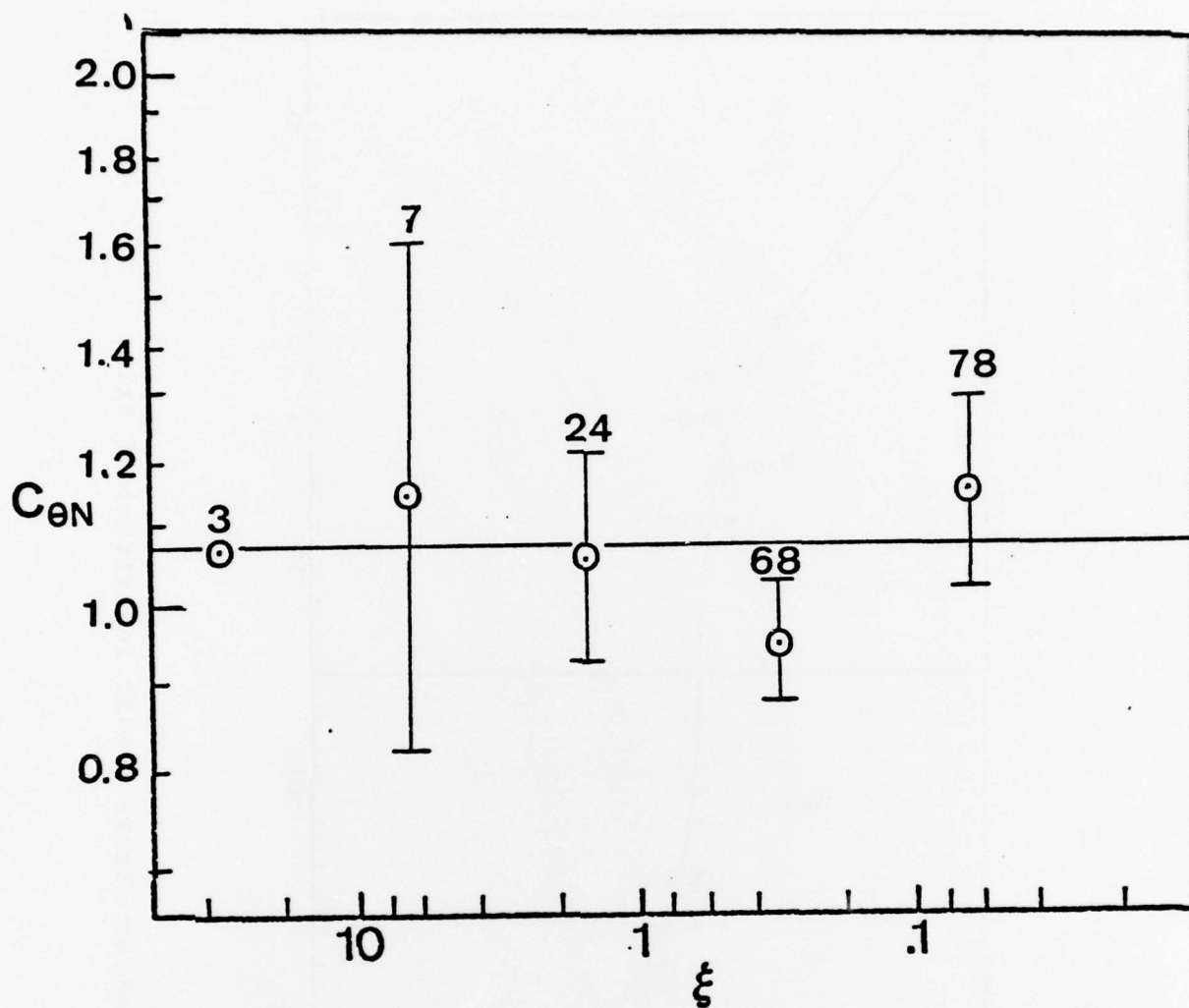


Figure 7.  $C_{\theta N}$  versus  $\xi$  results.  $C_{\theta N}$  based on Eq. 17 and CEWCOM-78 results.

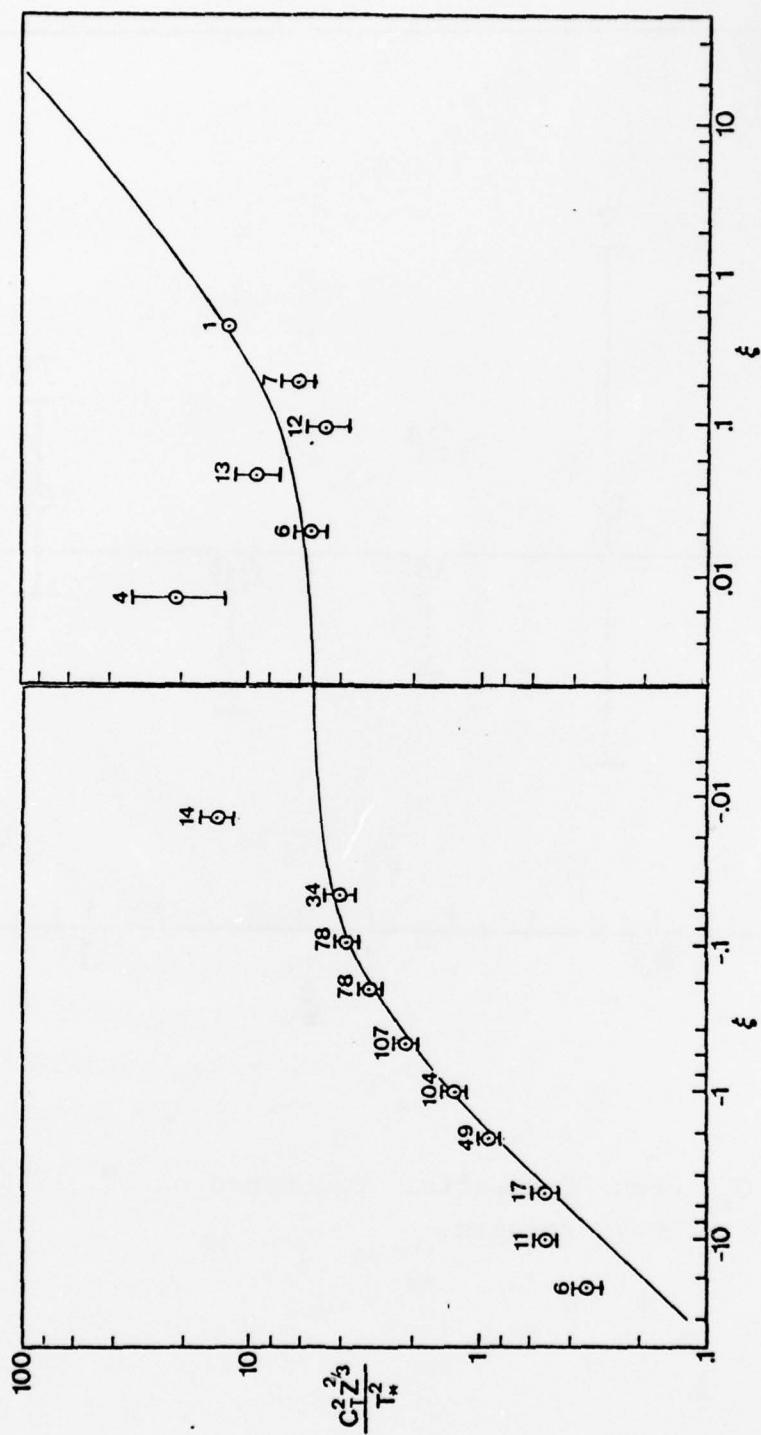


Figure 8. Same as Figure 6 with logarithmic  $\xi$  axis.



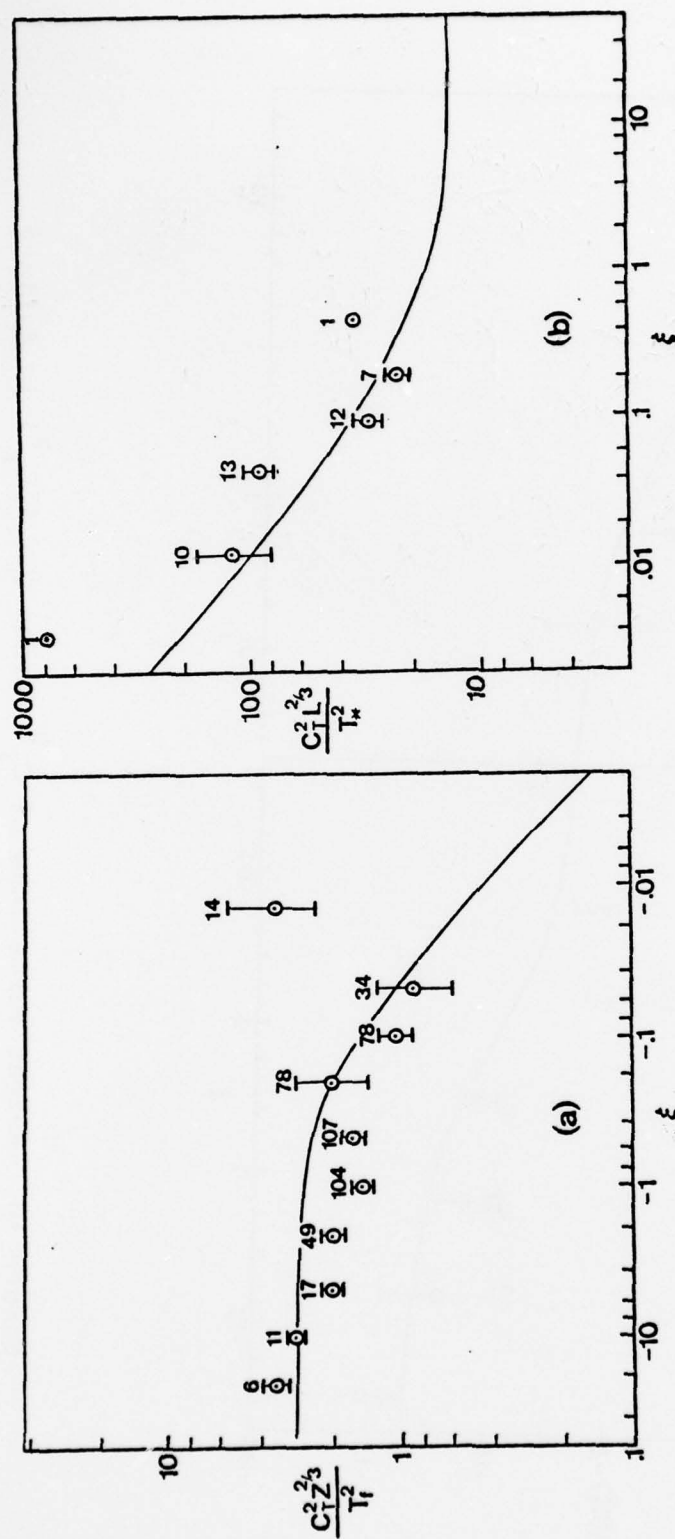


Figure 9. DTSP based on asymptotic scaling. (a) free convection curve is approximate prediction, Eq. 18 and, (b) Z-less, curve is prediction, Eq. 19.

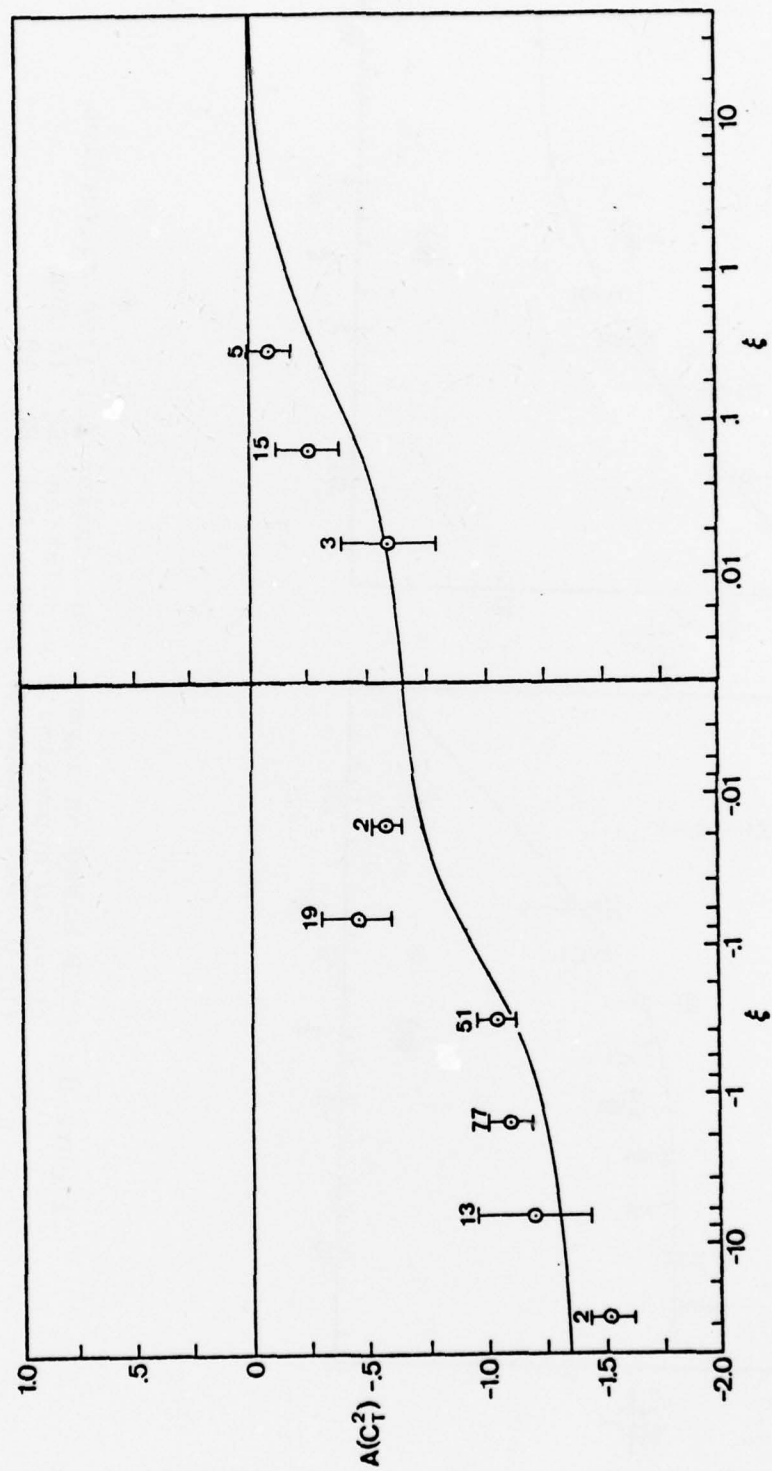


Figure 10. Height variations of  $C_T^2$  versus  $\xi$ .  $A(C_T^2)$  is defined by Eq. 20, solid curves are prediction based on Eq. 5.

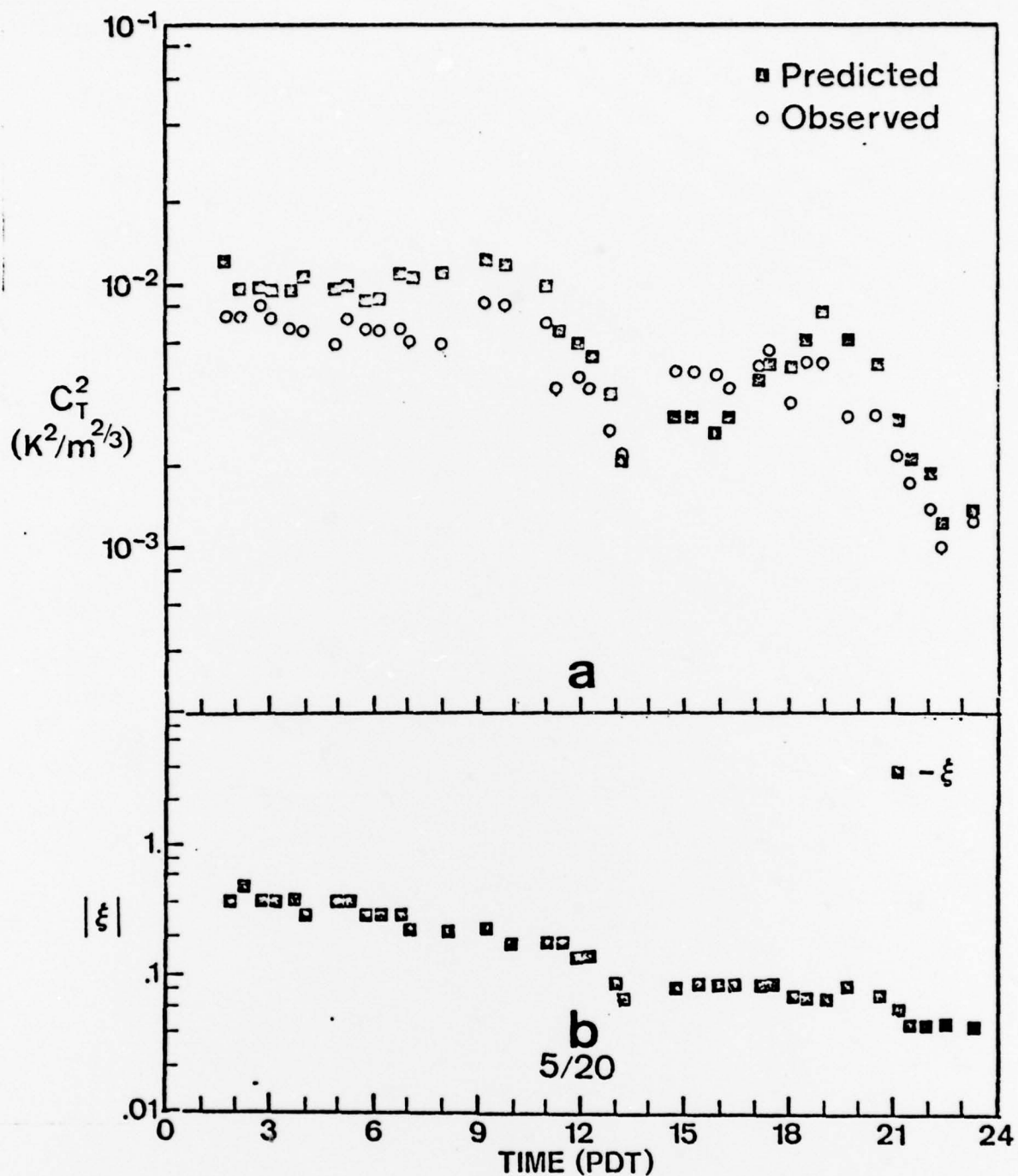


Figure 11. Results from 24 hour period during CEWCOM-78  
 (a) Observed and Predicted  $C_T^2$  for 10 meters  
 (b) Observed  $\xi$ .

# INITIAL DISTRIBUTION LIST

	No. of Copies
1. Defense Documentation Center Cameron Station Alexandria, Virginia 22314	2
2. Library, Code 0212 Naval Postgraduate School Monterey, California 93940	2
3. Dean of Research, Code 012 Naval Postgraduate School Monterey, California 93940	1
4. Asst. Professor C. W. Fairall, Code 61Fr Naval Postgraduate School Monterey, California 93940	5
5. Professor K. E. Woehler, Code 61Wh Naval Postgraduate School Monterey, California 93940	1
6. Dr. Ralph Markson Airborne Research Associates 46 Kendal Common Road Weston, Massachusetts 02193	1
7. Assoc. Professor K. L. Davidson, Code 63Ds Naval Postgraduate School Monterey, California 93940	5
8. Assoc. Professor T. Houlihan, Code 69Hm Naval Postgraduate School Monterey, California 93940	5
9. Assoc. Professor G. Schacher, Code 61Sq Naval Postgraduate School Monterey, California 93940	5
10. Mr. Murray Schefer Code Air-3706 Naval Air Systems Command Washington, D. C. 20360	1
11. LT Michelle Hughes PM-22/PMS 405 Naval Sea Systems Command Washington, D. C. 20362	1

No. of Copies

12. Dr. Stuart Gathman  
Code 8326  
Naval Research Laboratory  
Washington, D. C. 20375 1
13. Dr. Lothar Rohnke  
Code 8320  
Naval Research Laboratory  
Washington, D. C. 20375 1
14. Dr. Barry Katz  
Code 231  
Naval Surface Weapons Center  
White Oak Laboratory  
Silver Spring, Maryland 20910 1
15. Professor Dale Leipper, Code 68Lr  
Naval Postgraduate School  
Monterey, California 93940
16. Eugene J. Mack  
Calspan Corporation  
Buffalo, New York 14221 1
17. Theodore V. Blanc  
Code 8322B  
Naval Research Laboratory  
Washington, D. C. 20375 1
18. Dr. J. H. Richter  
Code 813  
Submarine Systems Division  
Communications Systems and Technology Department  
Naval Oceans Systems Center  
San Diego, California 92152 1